Multi-angle backscatter classification and sub-bottom profiling for improved seafloor characterization

Alevizos, Evan; Snellen, Mirjam; Simons, Dick; Siemes, Kerstin; Greinert, Jens

DOI
10.1007/s11001-017-9325-4

Publication date
2017

Document Version
Final published version

Published in
Marine Geophysical Research

Citation (APA)
Alevizos, E., Snellen, M., Simons, D., Siemes, K., & Greinert, J. (2017). Multi-angle backscatter classification and sub-bottom profiling for improved seafloor characterization. *Marine Geophysical Research*, 1-18. Advance online publication. https://doi.org/10.1007/s11001-017-9325-4

Mar Geophys Res (2018) 39:289–306
DOI 10.1007/s11001-017-9325-4

ORIGINAL RESEARCH PAPER

Multi-angle backscatter classification and sub-bottom profiling for improved seafloor characterization

Evangelos Alevizos[1,2] · Mirjam Snellen[2,3] · Dick Simons[2] · Kerstin Siemes[2] · Jens Greinert[1]

Received: 9 June 2016 / Accepted: 1 June 2017 / Published online: 8 June 2017

Abstract This study applies three classification methods exploiting the angular dependence of acoustic seafloor backscatter along with high resolution sub-bottom profiling for seafloor sediment characterization in the Eckernförde Bay, Baltic Sea Germany. This area is well suited for acoustic backscatter studies due to its shallowness, its smooth bathymetry and the presence of a wide range of sediment types. Backscatter data were acquired using a Seabeam1180 (180 kHz) multibeam echosounder and sub-bottom profiler data were recorded using a SES-2000 parametric sonar transmitting 6 and 12 kHz. The high density of seafloor soundings allowed extracting backscatter layers for five beam angles over a large part of the surveyed area. A Bayesian probability method was employed for sediment classification based on the backscatter variability at a single incidence angle, whereas Maximum Likelihood Classification (MLC) and Principal Components Analysis (PCA) were applied to the multi-angle layers. The Bayesian approach was used for identifying the optimum number of acoustic classes because cluster validation is carried out prior to class assignment and class outputs are ordinal categorical values. The method is based on the principle that backscatter values from a single incidence angle express a normal distribution for a particular sediment type. The resulting Bayesian classes were well correlated to median grain sizes and the percentage of coarse material. The MLC method uses angular response information from five layers of training areas extracted from the Bayesian classification map. The subsequent PCA analysis is based on the transformation of these five layers into two principal components that comprise most of the data variability. These principal components were clustered in five classes after running an external cluster validation test. In general both methods MLC and PCA, separated the various sediment types effectively, showing good agreement (kappa >0.7) with the Bayesian approach which also correlates well with ground truth data ($r^2 > 0.7$). In addition, sub-bottom data were used in conjunction with the Bayesian classification results to characterize acoustic classes with respect to their geological and stratigraphic interpretation. The joined interpretation of seafloor and sub-seafloor data sets proved to be an efficient approach for a better understanding of seafloor backscatter patchiness and to discriminate acoustically similar classes in different geological/bathymetric settings.

Keywords Acoustic backscatter · Angular response analysis · Bayesian statistics · Sediment classification · Sub-bottom

✉ Evangelos Alevizos
ealevizos@geomar.de

[1] GEOMAR Helmholtz Center for Ocean Research, 24148 Kiel, Germany

[2] Acoustics Group, ANCE, Department Control and Operations, Faculty of Aerospace Engineering, Delft University of Technology, Kluyverweg 1, 2629 Delft, The Netherlands

[3] Deltares, Princetonlaan 6, 3584 Utrecht, The Netherlands

Introduction

Acoustic mapping of seafloor sediments

The applicability and effectiveness of multibeam echosounder systems (MBES) in mapping seafloor sediments has improved significantly in recent years. By characterizing the seafloor in terms of its geo-acoustic properties, several studies have mapped benthic habitats (e.g. Brown and

Blondel 2009; Brown et al. 2011). In general this approach exploits the affinity of benthic species for seafloor areas that exhibit certain sediment properties, particularly grain sizes or hardness of the sediment. These correlate to acoustic properties that correspond to particular backscatter intensity levels (Collier and Brown 2005; Fonseca and Mayer 2007; McGonigle and Collier 2014). Other examples for habitat mapping using acoustic information are given e.g. in Blondel et al. (2006) who applied a multi-frequency approach to map deep sea corals; Ierodiaconou et al. (2007) combined video and image analysis with MBES data for mapping algae and invertebrate biotopes; Le Bas and Huvenne (2009) investigated various methods for processing acoustic data for benthic habitat mapping and Che-Hasan et al. (2012a, b, 2014) used Angular Response Analysis (ARA) for classifying the seafloor and link this to benthic habitats. Additional to studies using seafloor backscatter, others integrated backscatter with sub-bottom profiler (SBP) data as an approach for seafloor characterization. Sweeney et al. (2012) utilized MBES backscatter and high resolution CHIRP data for interpreting a low backscatter feature on the New Jersey (USA) continental margin, whereas Fakiris et al. (2014) combined side-scan sonar data with 3.5 kHz SBP data for benthic habitat mapping in the Lourdas Gulf (Greece). Siemes et al. (2010) used sub-bottom profiler data to investigate the reason for high seafloor backscatter data in areas with very fine sediment. The SBP data indicated the presence of gas in the area, which increase the measured seafloor backscatter strengths. Another example is given by Schneider von Deimling et al. (2013) who applied ARA on low frequency MBES data in conjunction with SBP data for identifying gas layers in the sediment of Eckernförde Bay (Germany). This shows that MBES and SBP datasets can complement each other for a better seafloor and sub-bottom property understanding. Acoustic seafloor classification results can be characterized further by correlating them to ground truthing but also SBP data if sub-seafloor reflectors have an expression on the seafloor, i.e. are partially exposed.

Objectives

This study investigates the usefulness of within-angle and between-angle variability of MBES backscatter values for seafloor classification based on MBES backscatter data derived from high density seafloor soundings. We apply a Bayesian probability method on backscatter values for each incidence angle and we compare its results against classification results based on multi-angle backscatter layers using Maximum Likelihood Classification (MLC) and Principal Components Analysis (PCA). The Bayesian method uses the backscatter measurements per beam and classifies sediments at the resolution of the average beam footprint. Information about the backscatter angular response is not directly used; however the angular dependence (influence of the grazing angle) of the backscatter must not be removed from the data. In contrast to that, the traditional Angular Response Analysis (ARA) matches the measured angular responses to a set of modelled angular response curves by varying the model input parameters until a maximum match is obtained. Traditional ARA results show only low spatial resolution since in most cases ARA is based on a fit of half of the swath of the MBES. In addition absolute backscatter strengths and thus well-calibrated MBES systems are needed for these backscatter measurements. In practice, backscatter measurements are often subject to imperfect calibration.

To counteract these drawbacks, we propose using empirical ARA (Beyer et al. 2007). This method is not dependent on absolute backscatter measurements and uses seafloor patches that are significantly smaller than half the swath width, which is considered a novelty in the field of backscatter processing and interpretation. The empirical ARA is based on stable, but not absolute backscatter measurements and is applied as an alternative to traditional ARA because of its insensitivity to systematic biases (Lurton and Lamarche 2015) and thus offers better backscatter processing opportunities for seafloor classification. Hughes Clarke (1994) and Parnum (2007) highlight the necessity that data for ARA should ideally be derived from small scale homogeneous patches of the seafloor to better resolve sediment differences. The strategy most often used to maximize class separability in traditional ARA studies is to combine them with backscatter mosaic segmentation results (Fonseca et al. 2009; Che-Hasan et al. 2012a, b; Rzhanov et al. 2012). Angular responses derived from segments representing homogeneous acoustic types are assumed to provide better discrimination capability. However, segmentation of backscatter mosaics relies on subjective settings selected by the user which has at the end implications for the selection of soundings belonging to a segment specific ARA response. In this study, we set the minimum dimensions of seafloor patches for extracting the ARA to 5×5 m assuming that within these patches sediment variability is minimal/not existing. This selection is justified by the high density of soundings per seafloor unit.

By comparing the performance of the different backscatter classification approaches we aim to test their suitability in resolving a wide range of sediment types using only the raw backscatter data and their angular dependence. Classification results are being assessed and characterized using grain size and SBP data.

Methodology

Study area

Eckernförde Bay (Eck Bay) has a diverse marine ecosystem and has been partially assigned as Site of Community Importance (SCI) under the Nature 2000 habitats directive. The study area has two basins with maximum depths of 20–30 m separated by the Mittelgrund area, a local elevation feature with a minimum depth of 8 m. Approximately 99% of the slope values in the entire area range between 0 and 5 degrees, which translates into a smooth seafloor morphology.

The entire area shows a high variability of sediment types, ranging from coarse sand with pebbles and boulders to silty clay. According to Jensen et al. (2002), Mittelgrund represents a relict morainic sill and is composed of glacial and marine sediments with variable thicknesses; predominantly Mittelgrund consists of glacial till and sands (Jensen et al. 2002).

Earlier geological, geochemical and geophysical studies in the area showed that the marine continuation of a glacial sand aquifer is responsible for freshwater seepage at places where the overburden sediments are not sealing due to coarser grain sizes (Jensen et al. 2002; Müller et al. 2011). Whiticar (2002) realized that the presence of pockmarks in Eck Bay is caused by this freshwater seepage and not, as suggested for several other pockmarks, by methane ebullition (Hovland and Judd 1988). In general, the southern part of the bay is formed by an incised channel filled with sediments of several meters of thickness whereas the northern part of the bay holds sediments with a vertical extent that could not be determined by the performed sub-bottom profiling because of gas blanking with free gas accumulating 1–2 m below the seafloor (see also Jensen et al. 2002). The deeper parts of the bay contain finer sediments (mainly silt) under highly anoxic geochemical conditions due to high organic matter concentrations (Whiticar 2002). Nittrouer et al. (1998) and Bentley et al. (1996) described the fine-scale stratigraphy of the deeper parts as areas in which most of the sediment consists of pelletized layers between 1 and 10 cm thickness alternating with slightly coarser (10% silt-sand) storm layers. Consequently, the study area contains a broad spectrum of seafloor sediment types, which in conjunction with the smooth seafloor bathymetry offers a excellent opportunity for dedicated MBES backscatter studies.

Multibeam data

The study area was surveyed using MBES between 2012 and 2015 onboard RV Alkor and RV Littorina. On both vessels, an ELAC Seabeam 1180 MBES was used operating at 180 kHz. The surveys mainly covered the wider area of Mittelgrund whereas towards the west the data get sparser. In particular the 2012 surveys covered a narrow 1×10 km corridor from the northern part of Mittelgrund to the northernmost coast of Eck Bay with a dense line spacing (20–50 m) as part of a 3D seismic survey. This survey plan yielded dense soundings per seafloor area for various incidence angles (Fig. 1). The MBES data were corrected for sound speed and tidal effects using the ELAC-HDPPost software. The complete processed data were exported as ASCII data for further analyses in GIS software packages. In addition raw backscatter data for each beam were extracted from the sonar files. They were used for acoustic classification using two unsupervised and one supervised methodologies; these are described below. The bathymetry grid and the backscatter mosaic of the area were generated using a 2 by 2 m cell size.

Bayesian unsupervised classification based on individual beam angles

The raw backscatter data were processed in Matlab using the unsupervised Bayesian classification technique developed by Simons and Snellen (2009) and Amiri-Simkooei et al. (2009). This technique is based on the central limit theorem; applied to backscatter analysis, this means that the backscatter intensities of a specific type of seafloor will have a Gaussian distribution when examined at a single beam angle or a number of adjacent beam angles. This technique fits a number of Gaussian curves to the histogram of backscatter values recorded for the beam(s) under consideration over the entire study area. For areas with more than a single sediment type, the total backscatter histogram can be approximated by a number of Gaussian curves, each Gaussian corresponding to a certain sediment type. To find the number of Gaussians that are minimally needed to obtain the best possible agreement between the measured and the modelled histograms, the x^2 criterion regarding the best fit to the entire histogram is considered. The minimum number of Gaussian curves that satisfy the x^2 criterion, represents the optimum number of classes that can be discriminated based on the backscatter response (Amiri-Simkooei et al. 2009; Siemes et al. 2010; Snellen et al. 2013). For determining this number, outer beams at about 40° incidence angle are considered because the number of scatter pixels in the beam footprint is high, resulting in the best possible discrimination of sediment types. The derived number of Gaussian curves is then used to fit the histograms for all other incidence angles. Based on the resulting fits, acceptance regions of backscatter values are obtained for each incidence angle (or set of adjacent beams grouped as 'one' incidence angle) by applying the Bayes decision rule for multiple hypotheses. Each acceptance

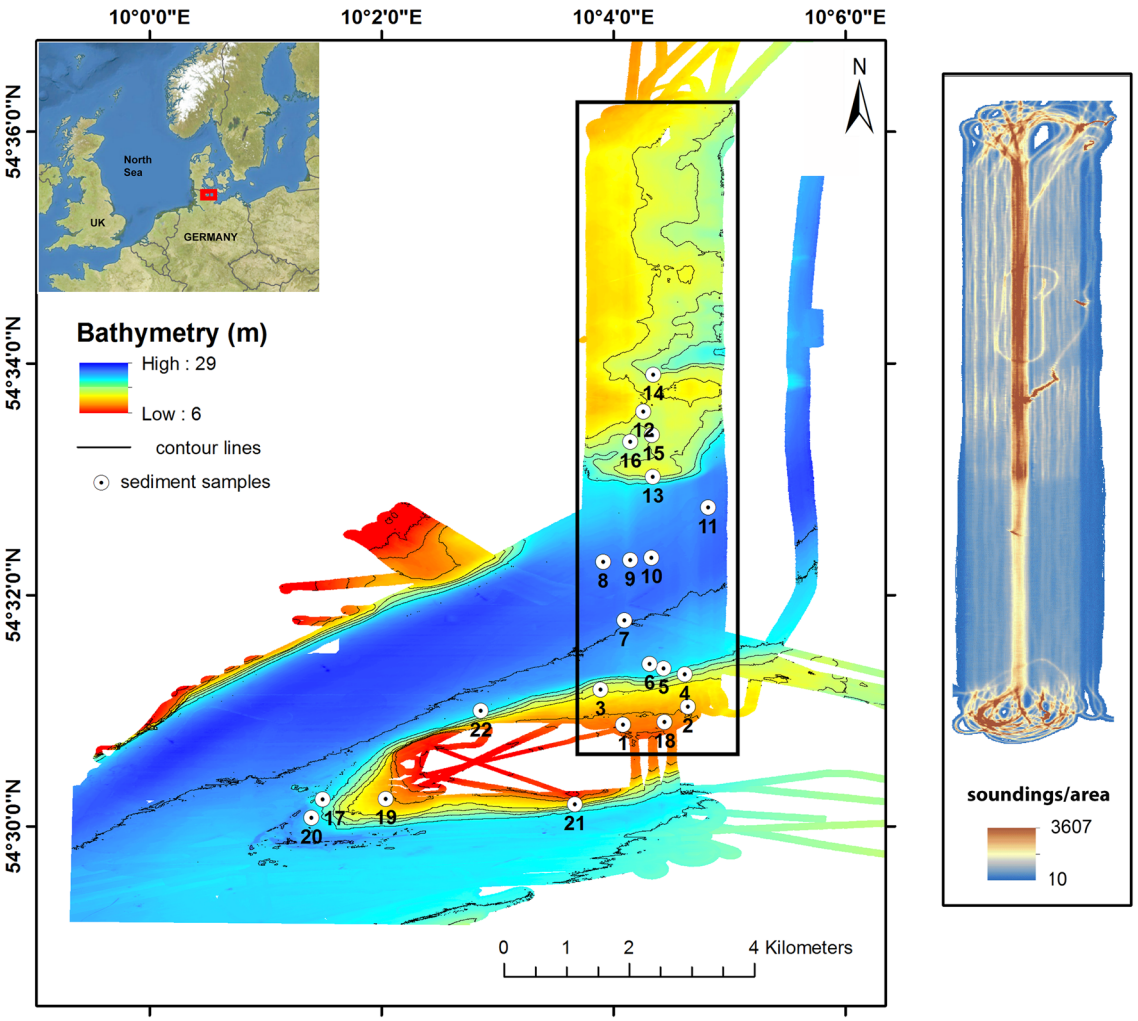

Fig. 1 Overview map of the study area with bathymetry and contours, sediment samples locations, and the high density line-spacing survey (*black rectangle*). Soundings in the legend of the right image refer to a 5×5 m area

region corresponds to a certain acoustic class. The main advantages of this technique are: (1) that no absolute sonar calibration is needed, (2) that it accounts for ping-to-ping variability, (3) that it can resolve different seafloor characteristics along the swath and (4) that it performs a statistical control on the optimal number of seafloor classes. A detailed description for applying the Bayesian approach to classify soft sediments can also be found in Alevizos et al. (2015). The final class assignment is performed for each beam and results can be exported as ASCII files and further analysed in GIS software packages.

Empirical angular response analysis and MLC based on angular layers

The angular dependence of seafloor backscatter varies with the physical properties of the substrate (Fonseca and Mayer 2007) and this has been used in many studies providing semi-quantitative information on surficial sediment properties (Beyer et al. 2007; Lamarche et al. 2011; Rzhanov et al. 2012; Huang et al. 2013). Although the methodology constitutes a robust and physical model approach, it tends to lack sufficient spatial resolution when applied to most MBES datasets. Since half of the sonar swath is usually considered as a single measurement for ARA, the resulting classification patches are at least a few tens of meters in size, even in shallow water (in 10 m water depth half of a 130° wide swath is 22 m). In addition, the traditional ARA approach requires MBES calibration. In the literature, approaches have been presented to compensate for these drawbacks; empirical approaches have been examined (Beyer et al. 2007) and strategies have been suggested to improve the spatial resolution of ARA (Fonseca et al. 2009). In this study, we follow an alternative approach that exploits the high sounding density of the used MBES surveys (Fig. 1) for extracting and utilizing

the backscatter angular dependence without losing spatial resolution. The high density of the seafloor ensonification in most of the study area allowed the extraction of angular backscatter measurements from selected 5×5 m seafloor patches (training areas) which are assumed to have a homogeneous sediment cover. Each of these patches includes several hundreds of evenly spaced soundings (Table 4, "Appendix"). The selection of seafloor patches was based on existing ground truth data (sediment samples) and the results of the Bayesian classification (Fig. 2). The high geo-acoustic resolution of the Bayesian approach (Alevizos et al. 2015) produces acoustic classes that discern minor differences between similar sediment types. In this regard, each extracted angular profile has a unique geometry representing different types of sediment (Fig. 2; Table 4, "Appendix"). Instead of the traditional ARA, where the full measured angular profile is used for a fit with a modelled angular profile, here we use the empirical ARA. The scheme for the resulting supervised acoustic classification was developed analogous to multispectral imagery classification. The measured backscatter intensity was gridded into individual layers, using the Inverse Distance Weighted (IDW) algorithm on the data points from individual beams at 20, 30, 40, 50 and 60 degrees of beam incidence angle (Fig. 2). In the end, five angular backscatter intensity layers with 5×5 m grid cell size were produced for the same area with small differences in overlap due to variable beam coverage. These layers were classified using the Maximum Likelihood Classification (MLC) algorithm implemented in ArcMap. The MLC considers that backscatter intensity values of a certain seafloor type follow a Gaussian distribution. This applies for most of our training sample data (Table 4, "Appendix") given that they are derived from local homogeneous areas.

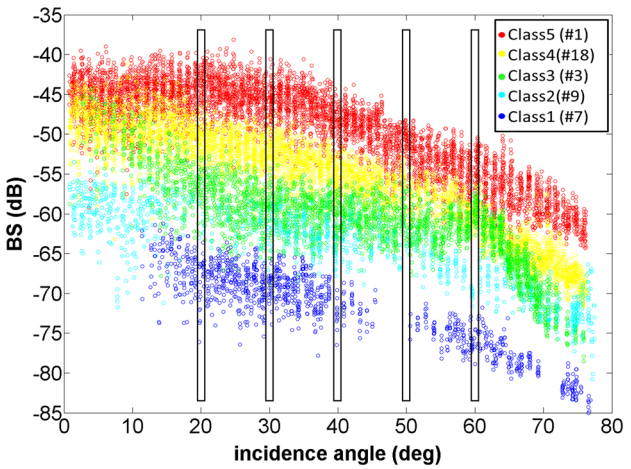

Fig. 2 Angular responses plot of selected 5×5 m patches belonging to different acoustic sedimentary classes. Ground-truth sample number in brackets indicates from which locations the responses were extracted. These were used as training areas (a priori knowledge) for the MLC. *Black rectangles* indicate the selected angles for producing the angular layers

The MLC algorithm is commonly used for multispectral satellite image classification and is also applied in seafloor mapping. Erdey-Heydorn (2008) and Calvert et al. (2014a, b) applied MLC in order to classify benthic habitats using multiple layers of bathymetry, bathymetric derivatives and backscatter data. The supervised approach chosen in this study is similar to the approach described in Che-Hasan et al. (2012b) who used 71 individual angular response layers with a set of supervised algorithms including the MLC. They considered half of the sonar swath for the ARA whereas in this study angular data from 5×5 m patches (training areas) are used in the MLC as a priori knowledge.

Because data acquisition in 2012 and 2014–2015 took place with different sonar configurations, we performed a comparison before classification. The comparison (Fig. 3) was based on separate examinations of soundings from two seafloor patches (5×5 m) with different sediment types that have been surveyed in 2012 and 2014–2015. These two patches were the only places sufficiently ensonified during all previous surveys. Although using two patches only may not be sufficient for statistical assessment of all ground truth locations, they provide an indication regarding the stability of the backscatter measurements over the different years and surveys. After validating the backscatter stability for two different seafloor types (gravel and sand) we hypothesize that the stability also holds for other seafloor types in the study area.

Principal components analysis using angular layers

This method is derived from satellite image analysis and allows for utilizing a dimensionally reduced dataset (fewer layers of information) to describe the data variability in a more effective way. The basic concept is to use a set of spatial layers as input and transform them into a new uncorrelated set of layers via orthogonal linear transformation of the initial set of layers. The transformed layers are fewer in number and represent an ordinal set of principal components. The first two principal components often account for the maximum in data variability and thus can be classified using a standard clustering algorithm such as k-means. The principal components do not contain the clusters themselves, but their combination has the potential for producing clustering patterns. Before the use of k-means, a cluster validation test is performed to estimate the optimal number into which the principal components can be clustered. The Principal Component Analysis (PCA) has been repeatedly applied for seafloor classification using acoustic datasets. One example is the study of Preston (2009), who applied PCA to a set of textural layers produced from MBES

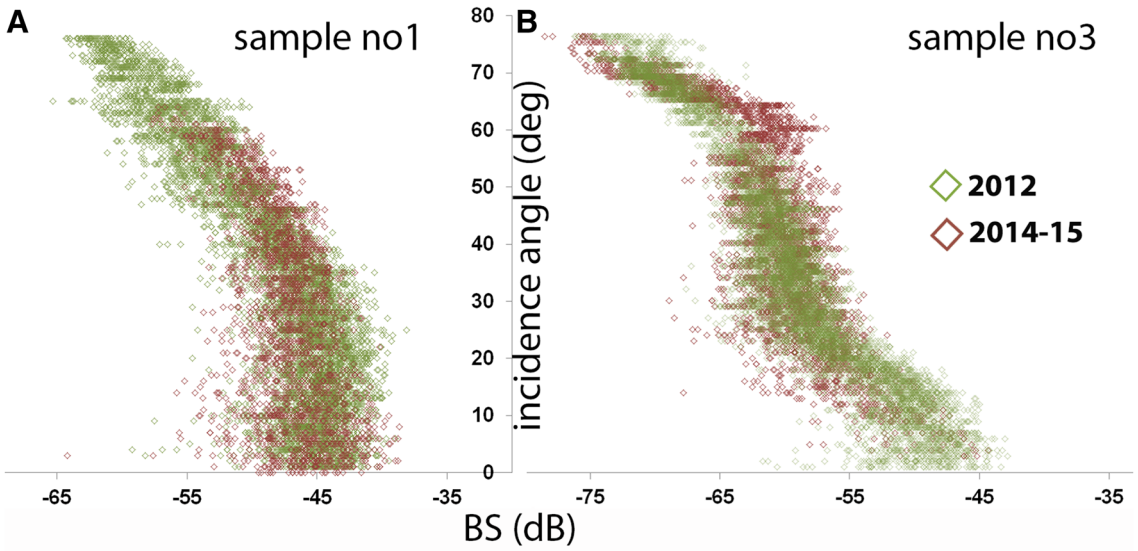

Fig. 3 Comparison between soundings from seafloor patches at sediment sample locations investigated during different surveys (2012 mobile SeaBeam 1180 on RV Alkor; 2014–2015 fixed installed SeaBeam 1180 on RV Littorina)

backscatter. Other examples are from Amiri-Simkooei et al. (2011) and Eleftherakis et al. (2014), who applied PCA to a set of MBES bathymetry derivatives and backscatter statistics to discriminate riverbed sediments. In the present study we apply PCA to the set of five MBES backscatter angular layers described above and use the first two principal components in conjunction with the k-means clustering algorithm to classify the seafloor. Cluster validation was performed using the C–H criterion (Calinski and Harabasz 1974).

Sub-bottom profiler data

A sub-bottom-profiler (SBP) survey in 2015 was designed to cover areas with variable seafloor backscatter responses seen in previous MBES surveys. The SBP survey was run with a SES-2000 system (Innomar) recording 12 and 6 kHz simultaneously with the Innomar SIS© software. The system was mounted at the side of the vessel on a stable pole. The acquisition occurred during good weather conditions; in total 25 km of SBP data including two profiles along the minor and major axes of the Mittelgrund were acquired (Fig. 4a). Pre-processing included applying a bandpass filter along with stacking and smoothing based on two consecutive traces for data enhancement and gain adjustment. In another step, the bottom reflector, the acoustic basement reflector, and the top of an acoustic turbidity reflector were digitized and exported for further analysis using Fledermaus 3D viewer. The term ‘acoustic basement’ is here referred to as the continuous reflector beyond which the acoustic signal does not penetrate any further. The digitized reflectors were further analyzed using ArcGIS and EXCEL. In particular, we used the SBP navigation to extract the depth and acoustic class information from the Bayesian classification results for the two along and across Mittelgrund SBP lines (Fig. 4a). Visual interpretation of the SBP data was enhanced by draping the classification results on the SBP profiles.

Sediment grain size analyses

Sample locations were selected by visual examination of the processed backscatter map (Fig. 4a) and acoustic classification results, with the aim of sampling as many different acoustic classes as possible for a robust validation. In total, 22 sediment samples were collected using a Van-Veen grab and a multi-corer. The samples were weighed and separated with 500 µm, 2 and 6.4 mm sieves. The fine fraction <500 µm was measured using a laser particle analyzer (Analysette-22 NanoTec, Fritsch©). We extracted the median and mode of each, the fine and total fractions and integrated the results of the particle analysis with the weight of the sieved fractions. This was achieved by converting the grain sizes of the fine fraction into weight assuming spherical particles.

Results

Backscatter analysis with the Bayesian approach indicates the existence of five acoustic classes (AC1-AC5, Fig. 4b, c). It is noteworthy that an intrinsic feature of the Bayesian classification is that it outputs sequential classes; here this means that an increasing class number represents

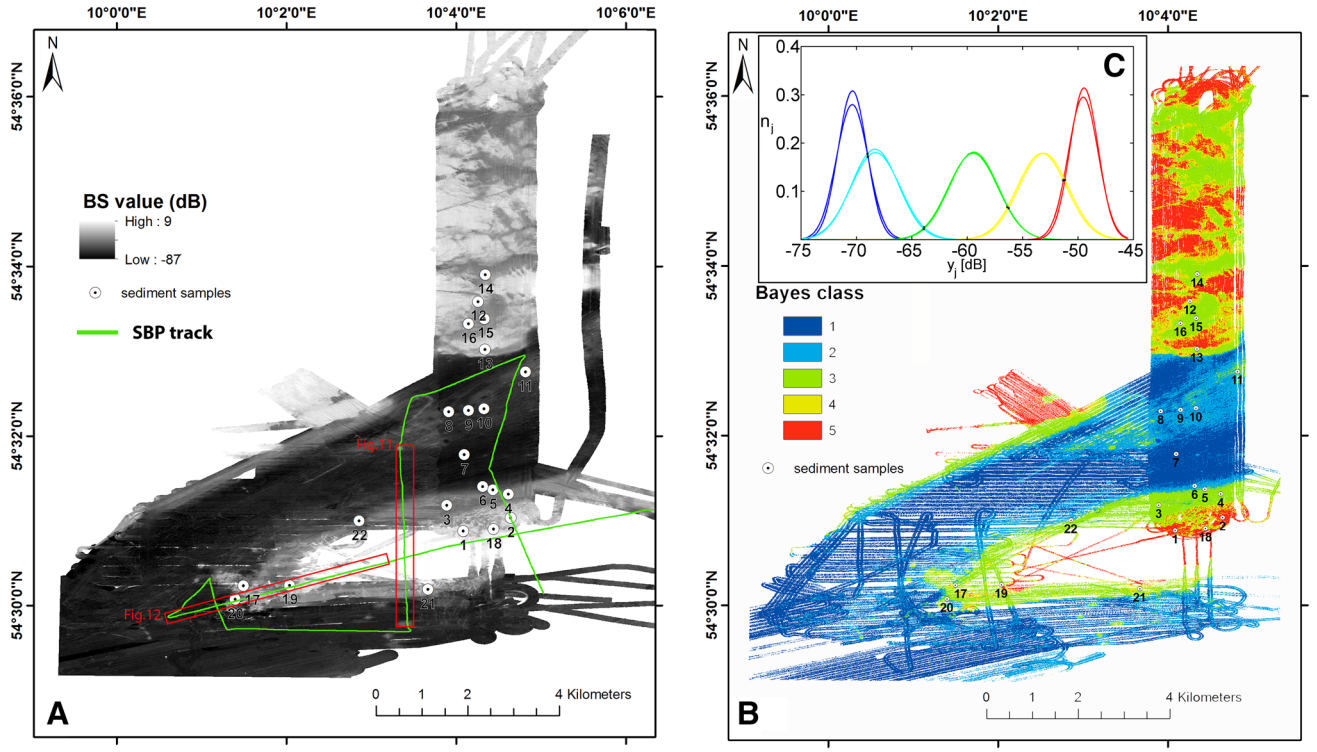

Fig. 4 **a** MBES backscatter mosaic of the study area (2012–2015 surveys) with sediment sample locations and SBP track lines (*green*). Red rectangles enclose the SBP profiles shown in the corresponding annotated figures. **b** Bayesian unsupervised classification map with locations of sediment samples. **c** Density functions fitted to the MBES backscatter raw data from beams with incident angles 38 and 40 (port side) representing five major acoustic classes (*curves* are *color-coded* for their respective classes). *Black squares* indicate the intersection points of adjacent curves

Table 1 Pearson's correlation coefficients for linear regressions of acoustic classes with grain size parameters

Grain size parameter	Correlation coefficient
Median (<500 µm)	0.71
Mode (<500 µm)	0.73
2–500 mm percentage	0.75
6.3–2 mm percentage	0.67

increasing backscatter intensity. Based on this we correlated the Bayesian classes against the derived grain size parameters (Table 1). Bayesian classes were also used for comparison with the classification results of the other two approaches and for the interpretation of the SBP data.

Bayesian classification and correlation with ground-truth data

The Bayesian method yielded five classes, expressed by Gaussian distributions holding a central dB value (Fig. 4c). The number of classes resulted from applying the x^2 criterion for the Probability Density Functions (PDFs) fitted to the backscatter histograms of beams with incidence angles of 38° and 40°. Using these two neighboring beams simultaneously for class validation, the robustness of the optimum number of classes is increased with better x^2 values and a better separation of the fitted PDFs (Fig. 4c). The suitability of incidence angles from the middle range of the swath is related to the significant different backscatter behavior of different sediment types in this range of incidence angles (for further explanation, see Discussion paragraph). The geo-acoustic resolution of the Bayesian classification (Alevizos et al. 2015) made it possible to map storm deposits within the upper ten centimeters of clayey/muddy sediment in the central area of the northern deep part of the Eckernförde Bay (samples 9, 10, 11, Fig. 4b) as the two separate acoustic classes AC2 and AC3. In general the sediments in the northern deep part have been described by Nittrouer et al. (1998) and Bentley et al. (1996) as sediments consisting of pelletized layers between 1 and 10 cm thickness alternating with slightly coarser storm layers (10% silt-sand).

Acoustic classes AC2 and AC3 (sediment samples 9 and 11) show only a small increase in coarse material (0.5–4%)

within a generally fine grained matrix (Table 5, "Appendix"). We interpret these as storm deposits in which the coarse fraction produces the slightly stronger backscatter in the central deep part of the bay.

In an additional step, each class was correlated with different parameters of the grain size results (median, mode, and coarse fraction percentages, see Table 1) validating the acoustic clustering. In particular the percentage of the coarse sand fraction (2 mm–500 µm) along with the mode and the median grain size of the fine fraction (<500 µm) show high correlation coefficients with the five classes (Table 1). However, the lower the class number (lower dB values) the greater is the ambiguity (class overlap between classes 1 and 2 in Fig. 4c).

ARA-MLC and PCA classification using multi-angle layers

The MLC algorithm used the angular information from soundings of homogeneous training areas (Fig. 2). The data of these training samples partially satisfy the basic assumption of the MLC concept that a particular sediment type expresses a normal distribution of backscatter values (Table 4, "Appendix"). Only samples from classes AC1 and AC2 show a different distribution, but these classes also hold much fewer data points. During the MLC processing, the mean vector (Fig. 5b) and the covariance matrix of all angular layers are estimated from the training set. This information is then used for assigning classes to the rest of the data. The clear separation of the angular backscatter response curves in Fig. 5b enhances the performance of the supervised classification, hence minimizing class overlap. The small standard deviation for class AC1 and AC4 might be responsible for the small areas assigned to these classes. It was found that AC4 occupies more small patches compared to the results of the two unsupervised methods (Fig. 5a, b) and shows a more abrupt transition from AC5 to AC3, particularly in the northern part of the bay. Data gaps in the final ARA-MLC classification map are due to unclassified pixels that did not hold sufficient overlap with all angular layers.

The PCA results were clustered in five classes (as derived from the C-H criterion) using the k-means algorithm (Fig. 5c). Figure 5d shows these five classes in which the first two principal components of soundings from the 5×5 m patches of all sediment sample locations are

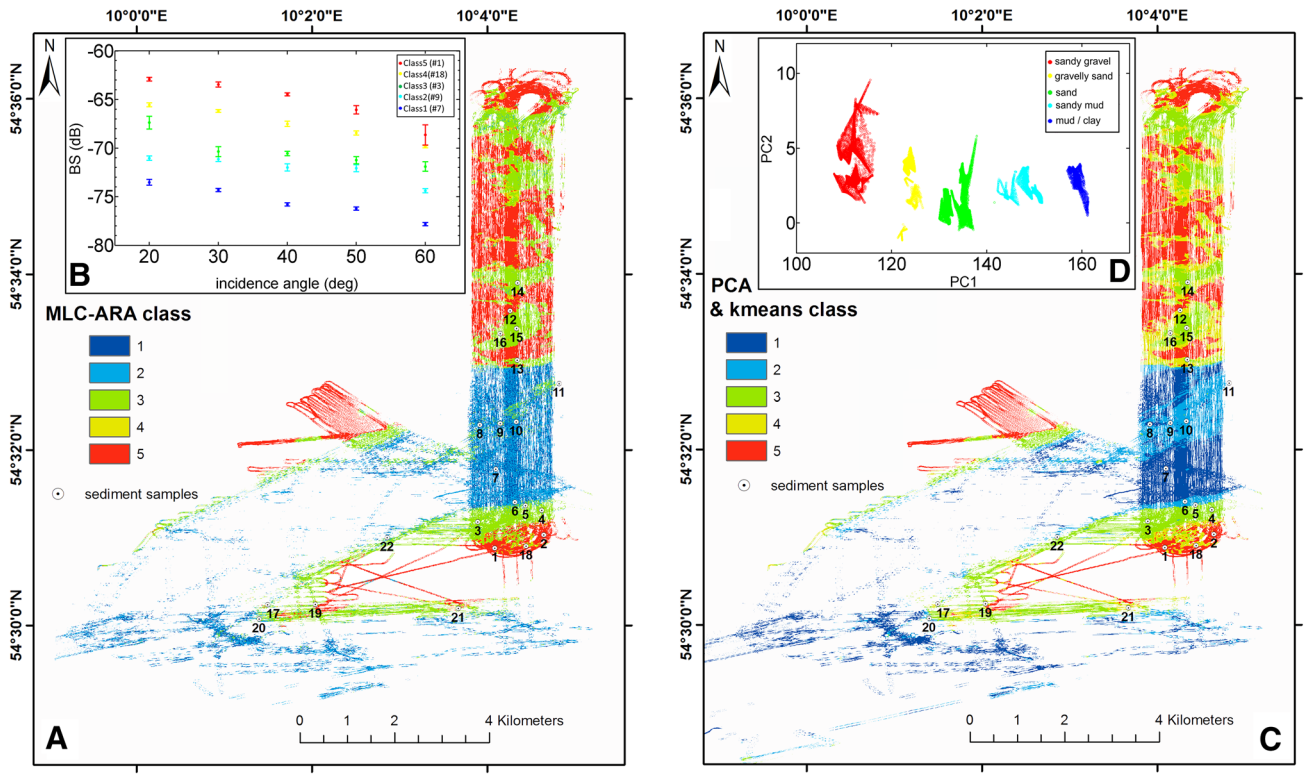

Fig. 5 **a** Classification map of the supervised ARA-MLC method with locations of sediment samples, **b** angular mean and standard deviation of backscatter values for each class of the training sample soundings. These data were derived from the "signature file" produced in ArcMap that is used by the MLC algorithm for assigning classes using the angular layers 20–60 degrees, **c** classification map of the PCA method clustered with the k-means algorithm including locations of sediment samples, **d** scatterplot of the first two principal components of soundings from all sediment sample locations. PC1 and PC2 resulted from the combination of five angular layers

plotted. The k-means clustering of the PCA results produced classes without ordinal character. It was observed that the spatial extent of each class corresponds very well with the spatial extent of the Bayesian classes that are ordinal. Hence the PCA and k-means classes were reclassified to correspond to the Bayesian ordinal classes order.

Acoustic class description and sub-bottom interpretation

SBP data show an acoustic basement with a continuous high-amplitude reflector. The depth of this reflector is lowest on top of Mittelgrund where it corresponds to the seafloor surface; it increases to 1–2 m along its slopes and rapidly deepens with increasing distance from the Mittelgrund (Fig. 6a). It is not possible to track the acoustic basement in the northern part of the bay because of gas blanking (Fig. 6a, symbol *g*), but we assume that acoustic basement lies several meters below the fine-grained sediment cover. Interpretation of the SBP data is supported by the Bayesian acoustic classes that correspond with the proximity of the acoustic basement to the seafloor (Fig. 7; Table 2); the shallower the depth of acoustic basement, the higher the backscatter intensity. This is rather related to geological factors and not to the limited (<10 cm) penetration of the high frequency (180 kHz) acoustic signal (Ferrini and Flood 2006). Three distinct acoustic layers can be identified between the seafloor and the acoustic basement. The uppermost acoustically transparent layer of 0.5–1 m thickness is found along the southern and northern flanks of Mittelgrund (Fig. 6a). Directly below, a 0.5–1 m thick layer with chaotic reflectors can be observed. This layer reaches the seafloor mainly on the shoulder of Mittelgrund, where it is locally covered by the uppermost acoustically transparent layer (Fig. 6a, enlargement). Away from Mittelgrund, a more than two meters thick layer with parallel reflectors covers the northern and southern basins of the bay. In the north, this layer is blanked by free gas accumulations approximately 2 m below the seafloor (Fig. 6a symbol *g*). Apart from continuous reflectors, sparse or dense hyperbolic reflectors were found as the uppermost acoustic layer in the westernmost part of Mittelgrund (Fig. 6b enlargement, symbol *h*).

When overlaying the Bayesian acoustic classes on the sub-bottom profiles, AC3 mostly overlays the transparent uppermost layer on the Mittelgrund flanks (Fig. 6a, b). AC4 corresponds with the outcrop of the chaotic reflector layer at the southern flank of Mittelgrund (Fig. 6a). Away from the flanks, AC4 corresponds to hyperbolic reflector layers (Fig. 6b, symbol *h*). It is assumed that AC5 (highest backscatter intensity) covers a large portion of the shallowest part of Mittelgrund, which mainly consists of glacial till. There is no layering visible in the SBP data from this area due to the very hard reflection at the seafloor surface (Fig. 6a, b). It should be noted that AC3 away from the Mittelgrund also appears as patches within AC2 (Figs. 4b, 6a). AC1 covers the deeper parts of the area and locally alternates with AC2. The top of the acoustically opaque layer in the northernmost part of the profile is highlighted in Fig. 6a. In the southern part, acoustic blanking occurs only locally in the deeper part of a paleo-channel (Fig. 6a).

In the following we present the characteristics of each Bayesian class along with their relationship to SBP interpretations and ground truth data following Folk's sediment classification (Folk 1954):

Acoustic class 1 (AC1) mud/clay

According to two ground-truth samples this class represents the top of anoxic mud and clay deposits covering mainly the deep parts of the study area, where thick (>2 m) sediment accumulations exist with parallel reflectors in SBP data (Fig. 6a).

Table 2 Summary sedimentological and acoustic description of the Bayesian classes (mbs: meters below seafloor)

Bayes class	Central dB value	Backscatt-ering factors	SBP units	% Coarse (>500 µm)	Jensen et al. (2002)	Depth of acoustic basement (mbs)
1	−70.3	Grain size	–	–	Littorina mud (with gas)	>>2
2	−68	Grain size	–	≤1	Littorina mud (with gas)	>>2
3	−61	Grain size, shells	Uppermost transparent layer	1–4.1	Late glacial sand (fine fraction)	0.5–2
4	−55.9	Grain size, epibenthos, shells	Chaotic layer, hyperbolae	15	Late glacial sand (coarse fraction)	0–0.5
5	−50.9	Grain size, epibenthos, shells	Acoustic basement	>>20	*Subsurface*: quaternary sand, *exposed*: Littorina sand and gravel/till	0 (or few cm)

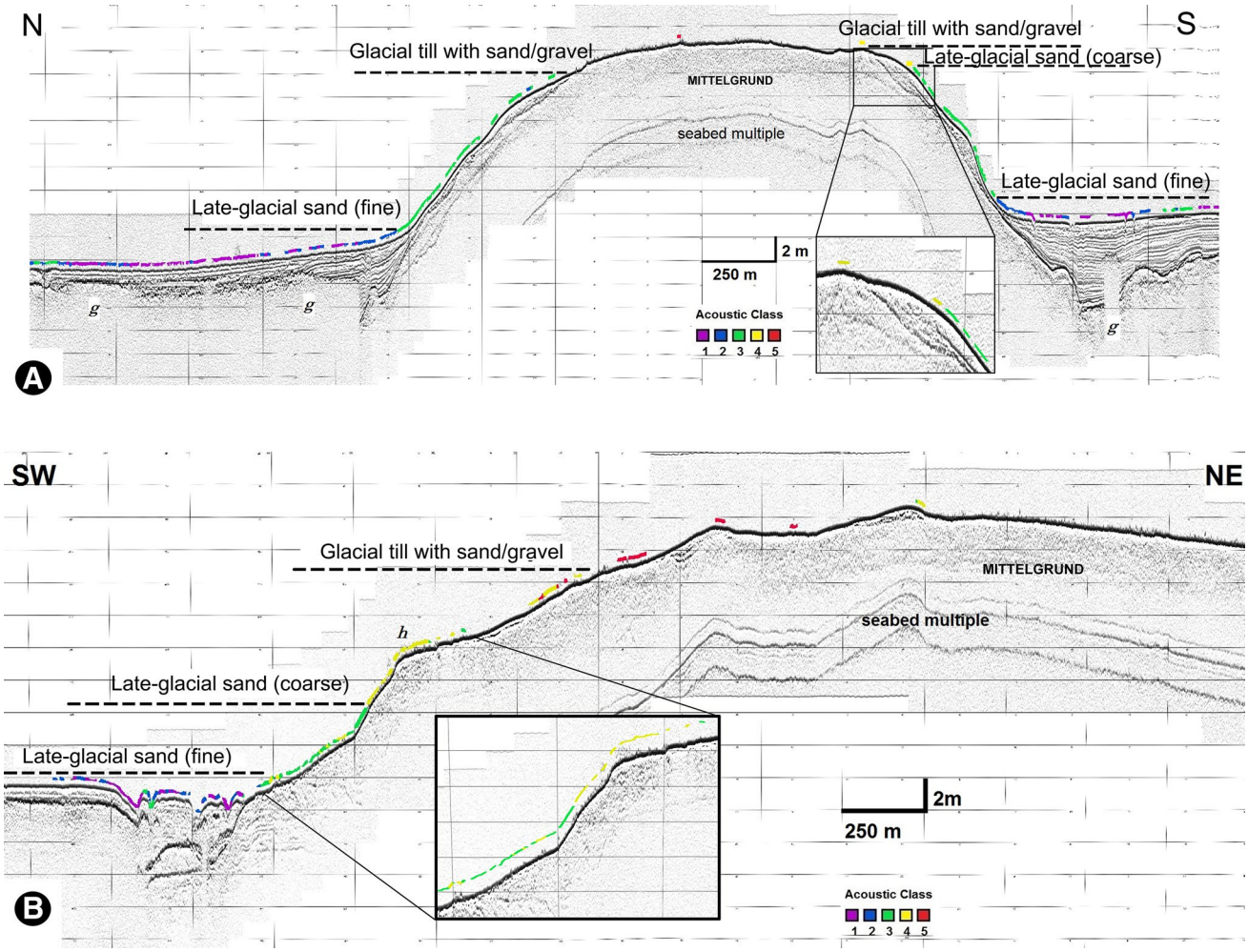

Fig. 6 **a** Sub-bottom profile (location on Fig. 4a) crossing the minor axis of Mittelgrund. In the southern part the incised paleo-channel is clearly visible, filled with a well layered sediment package. In the northern part, gas trapped in the upper 1–2 m of sediment (g) prevents the signal from penetrating into the deeper sediment layers (Jensen et al. 2002). Acoustic class 3 dominates the Mittelgrund flanks, **b** sub-bottom profile (location on Fig. 4a) along the western tip of Mittelgrund. Acoustic class 4 correlates to hyperbolic reflectors (symbol h, enlarged image)

Acoustic class 2 (AC2), gravelly/sandy mud

Based on grain size analysis of five samples, this class represents muddy and clayey sediment, similar to AC1, but holds a small percentage (<1%) of coarse grained material (including clasts, shells and shell fragments). This class is mainly found in the deep basin of the bay and at the foot of Mittelgrund.

Acoustic class 3 (AC3), sand

According to nine samples, this class consists of at least 80% fine sand (Table 2) with varying percentages (1–20%) of coarse sand and a small amount (<1%) of gravel-sized particles. Seafloor patches of this class are found in the deep basin, on the flanks of the Mittelgrund and within the pockmarks SW of Mittelgrund (Fig. 4b). According to the SBP data interpretation (Fig. 6a, b) class AC3 is characterized by the presence of a thin (up to 1 m) transparent acoustic layer on both the northern and southern flanks of Mittelgrund. Grab samples from this class consistently recovered bivalves (*Macoma balthica, Astarte sp.*), numerous tubes of *Pectinaria* worms and several *Ophioura* specimens. This indicates that the backscatter character of AC3 might also be affected by the presence of macro-benthos.

Acoustic class 4 (AC4), gravelly sand

Sediments of this class (four samples) include a moderate amount (5–30%) of coarse sand, a small amount of gravel (1–8%) as well as shells and occasionally pebbles in a medium sand matrix (>50%). This class is related to a thin

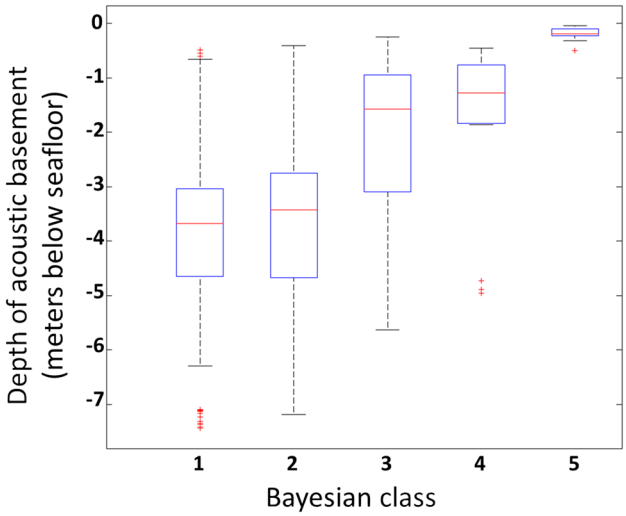

Fig. 7 Boxplot illustrating the relation of Bayesian acoustic classes to the depth of the acoustic basement below the seafloor

layer of chaotic reflectors outcropping at the southern part of Mittelgrund (Fig. 6a, b) and to the presence of hyperbolic reflectors at the westernmost slope of Mittelgrund (Fig. 6b, symbol *h*).

Acoustic class 5 (AC5) sandy gravel

Two sediment samples of this class are characterized by the coarsest sediments recovered from the study area, consisting of 30–40% medium sand, at least 60% coarse sand and 2–14% gravel. Shells and pebbles are also present in the samples and we assume that the top of Mittelgrund corresponds to the exposed acoustic basement (Fig. 6a, b).

Discussion

Angular response classification, comparison of single with multi-angle approaches

In this study we examine the within-angle and between-angles backscatter variability using different methods for defining seafloor acoustic classes with high spatial resolution. The Bayesian method is employed to estimate the optimum number of classes; this approach performs cluster validation before the final assignment of classes. This is an advantage compared to other unsupervised methods, which usually require some kind of external cluster validation tool (Verfaillie et al. 2009). However, the assumption of the Bayesian method—that the backscatter values within each seafloor type should have a Gaussian distribution—has been criticized because seafloor sediments or benthic habitats appear multi-modal by nature (Che-Hasan et al. 2012b). Sediment inhomogeneity in the study area is evident and different seafloor types can generate a similar backscatter response. For example, AC3 (sand) seems to be the same class as gravelly/sandy mud. The same is true for AC4; here the backscatter is the result of either boulders on the seafloor or coarse sediments from exposed layers. This ambiguity is also addressed in Eleftherakis et al. (2014). Therefore we suggest that combining various sensors such as MBES and parametric SBP along with sufficient ground truth data can offer a better discrimination of sedimentary classes.

In the study area the majority of the bathymetric surface has a slope of less than five degrees, so that no specific corrections of backscatter values are needed to account for the true grazing angle. This reduces pre-processing efforts considerably. The reference incidence angles used to drive the Bayesian classification lie in the mid-range of the MBES swath, this is in agreement with previous studies using the backscatter angular dependence (Lamarche et al. 2011; Hamilton and Parnum 2011; Che-Hasan et al. 2014) and also with studies using the Bayesian approach (Alevizos et al. 2015). The selection of middle range beams is well suited for obtaining a realistic number of classes (best fit of five Gaussian curves according to the x^2 criterion) and hence to reliably differentiate various seafloor types. The good performance of the Bayesian classification using incidence angles of 38° and 40° is also supported by Lamarche et al. (2011), stating that reliable backscatter measurements from angles closer to the nadir (<20°) are hindered by specular reflection that dominates the backscatter, whereas measurements in the outer range (>60°) are prone to strong angle dependencies and thus are less coherent.

Results from methods using angular layers (ARA-MLC and PCA) are compared to the Bayesian classification map which serves as reference, by examining their contingency matrices using Cohen's kappa as a measure of agreement. Usually contingency maps are produced by the combination of a classification map and a ground truth (reference) map for the same area. In this case the Bayesian classification map has the role of the reference map and is compared with the two multi-angle approaches. The relative agreement between the classes is assessed via the percentages of accurately classified pixels (Bayes_acc, PCA_acc and ARA-MLC_acc; Table 3) for each method. For the PCA and ARA-MLC methods, PCA_acc and ARA-MLC_acc represent the respective percentage of pixels in agreement with the Bayesian class, while Bayes_acc represents the reliability of this agreement. As an example from Table 3, 93% of the pixels classified as class AC1 by the PCA method are in agreement with the Bayesian results. As the Bayesian approach has 22% more pixels identified as AC1, the Bayes_acc value only gives 78% reliable agreement compared to the PCA classification for AC1. Additionally,

Table 3 Contingency matrices showing the number of pixels classified and the relative accuracy percentages for the three methods (numbers in bold: Bayes_acc, PCA_acc, and ARA_MLC_acc)

Bayes—PCA (kappa = 0.91)	Class 1	Class 2	Class 3	Class 4	Class 5	PCA_acc
Class 1	114,642	9054	13	0	0	0.93
Class 2	31,990	64,667	1769	2	0	0.66
Class 3	109	8285	121,610	27,591	86	0.77
Class 4	4	23	3607	62,012	24,605	0.69
Class 5	0	2	13	5261	114,517	0.96
Bayes_acc	0.78	0.79	0.96	0.65	0.82	
Bayes—ARA-MLC (kappa = 0.76)	Class 1	Class 2	Class 3	Class 4	Class 5	ARA-MLC_acc
Class 1	41,237	81,878	592	0	2	0.33
Class 2	26,179	60,997	11,249	0	3	0.62
Class 3	299	14,081	134,397	6182	2722	0.85
Class 4	2	1843	15,231	18,247	54,928	0.20
Class 5	1	534	145	985	118,128	0.99
Bayes_acc	0.61	0.38	0.83	0.72	0.67	

the agreement between the three methods can be assessed using the classification results for each sediment sample location in Table 5, "Appendix". The contingency tables show that both the PCA and MLC approach produce comparable results with good agreement relative to the Bayesian method (Table 3). However, there are some fluctuations in the agreement between some acoustic classes. The highest overall agreement occurs between the unsupervised methods (Bayes and PCA). We observed that for classes AC5 and AC4, the PCA method generally agrees with the Bayesian approach, whereas there are minor differences regarding the percentage of pixels classified as classes AC1 to AC3 (Table 3). In contrast, the ARA-MLC approach shows a lower degree of agreement with the Bayesian map, particularly for classes AC1 and AC4. Despite these observations, the high Cohen's kappa values indicate that seafloor patches were classified consistently and that class assignments do not occur by chance.

The high sounding density allowed producing separate backscatter mosaics from selected angles. Between 20 and 60 degrees incidence angle there is little overlap between adjacent angular profiles, so beam angles from that range were selected to produce angular layers used by MLC and PCA. In this regard, the Bayesian classification was useful in quantifying the separation between the angular responses, hence maximizing the discrimination capability of the training set for the MLC. This highlights that Bayesian classification and ARA are a good complementary tool set. The Bayesian approach examines backscatter variability along a "narrow corridor" of middle range incidence angles quantifying the difference between angular responses in a statistically robust way.

The combination of empirical ARA with the MLC algorithm provides an automated sediment classification tool that depends on acoustic properties of the seafloor area under investigation. Sufficient ground truth information is required for both the classification and validation processes. In this study, applying empirical ARA to data from non-calibrated MBES was possible because the angular response profiles of the different sediments were sufficiently separated (Figs. 2, 5b). The backscatter values for the areas of training samples 7 and 9 (for classes AC1 and AC2 respectively), are not normally distributed and they are considerably skewed (Table 4, "Appendix"). The less good performance of the empirical ARA-MLC method for these two classes can be interpreted as a result of lack of normal distribution which is a prerequisite for the MLC method. Che-Hasan et al. (2012b) suggested that the MLC method does not work for sediments with a high degree of homogeneity. However, it has to be mentioned that they incorporated 71 different variables in their MLC, while it has been suggested that MLC is not suitable for data with high dimensionality and using only a limited amount of training data (Benediktsson

et al. 1995). Considering our data, it is not clear whether the low performance of the empirical ARA-MLC method is an algorithm shortcoming or if a poor data quality is the reason. Once more, if training samples with continuous angular backscatter responses can be used, the performance of the MLC for sediment differentiation can be more reliably evaluated. It is also suggested that future studies should make use of more than five angular layers in order to examine the capability of MLC to adequately classify (better discriminate) similar seafloor types.

The PCA and k-means approach, based on multi-angle layer information appears to discriminate the different sediment types in the study area efficiently (Fig. 5d). Although the five angular layers are highly correlated ($r^2 > 92\%$), the resulting first two principal components are uncorrelated and describe more than 95% of the between-angle backscatter variability. The spatial correspondence and agreement between the Bayesian and PCA classification maps can also be assessed by their contingency matrix.

Joint interpretation of sub-bottom structures and seafloor acoustic classes

Overlaying the Bayesian acoustic classes on SBP data and considering the results from Jensen et al. (2002) and Whiticar (2002) a good understanding of the wider Mittelgrund area stratigraphy can be supported. Acoustic class AC5 near Mittelgrund, maps the exposed acoustic basement (Fig. 6a, b) of glacial till or Littorina sand and gravel as described by Jensen et al. (2002) (Table 2). Other acoustic classes could be attributed to specific sub-bottom layers that pinch out at the seafloor, determining the seafloor backscatter (Table 2). Jensen et al. (2002) suggest that only one sediment type covers the glacial till on the Mittelgrund flanks, whereas the acoustic classification of this study could define two different seafloor types on the flank areas. These two classes (AC3 and AC4) can be linked to a finer and coarser fraction of Late Glacial sand as identified by Jensen et al. (2002). In this respect the layer with a chaotic character reaching the seafloor in the proximity of the Mittelgrund shoulder is related to AC4, representing the coarser fraction of Late Glacial sand (Fig. 6a, enlargement). AC3 which is related to the upper transparent reflector that covers large part of the Mittelgrund flanks probably represents finer material from Late Glacial sand deposits and seems to be an important substrate for the local benthic communities. Jensen et al. (2002) describe these deposits as laminated or massive fine sand and silt that marks the transition into the basin. We assume that patches of AC3 in the deep basin (Fig. 6a) represent the coarser material of the storm deposits mentioned earlier (Nittrouer et al. 1998). AC3 also comprises the seafloor within the pockmarks SW of Mittelgrund (Fig. 6b) and vibrocore samples from within a pockmark in the same area (Jensen et al. 2002) confirm the existence of sand and gravel. Class AC1 can be simply characterized as Littorina mud (Jensen et al. 2002), but AC2 may be interpreted in two ways. Its occurrence at the foot of Mittelgrund is probably associated with deposits that are also characterized as Littorina mud whereas its appearance in the deep part of the basin possibly represents the finer fraction of sediments deposited during storms (Nittrouer et al. 1998).

Bayesian acoustic classes correlate with the maximum penetration depth of the SBP signal (the depth of the acoustic basement; Fig. 7). This paradoxical relationship between hydro-acoustic signals, with large difference in sediment penetration, highlights the connectivity of the two acoustic datasets in terms of their geological implications. It can be assumed that the depth of the acoustic basement is related to geological processes (e.g. transgressional erosion, sedimentation, reworking) that have taken place in the area and affect the coarseness of the surficial sediment. Accordingly, the variability in coarseness is reflected in the acoustic classification of the seafloor surface backscatter. It is inferred that areas with softer sediments allow a greater penetration of the SBP acoustic signal, which explains the relation between acoustic classes and acoustic basement.

Conclusions

Using gridded layers of MBES backscatter from various beam incidence angles proved useful for sediment class differentiation for both supervised and unsupervised approaches. These gridded layers were obtained from surveys resulting in high density soundings per seafloor area enabling to resolve acoustic classes in a higher spatial resolution than traditionally achieved. Single-angle analysis of raw backscatter data was performed using Bayesian statistics. This method performs cluster validation autonomously; the results correlated well with grain size analysis and provided a useful classification map for comparison with two multi-angle methods.

Combining multi-angle backscatter layers with empirical ARA-MLC gave promising results for discerning sediment

classes at high spatial resolution. This is particularly interesting, as traditional ARA methods lack spatial resolution. The high density of soundings in the area supported the extraction of distinct angular backscatter responses from smaller seafloor patches; compared to other ARA studies described so far, the resulting maps are significantly more detailed. This is an advancement of the traditional half-swath and BS mosaic segmentation approaches, maximizing the between-class separation.

The applied empirical ARA method could be applied to uncalibrated sonar data once the extracted angular measurements were consistent for each seafloor class/type, and clearly separated from each other. PCA using multi-angle layers resolved the same number of classes as the Bayesian approach, highlighting the consistency of results between all three approaches.

The incorporation of high resolution SBP data helped to characterize acoustic classes and added valuable information on the vertical and horizontal distribution of exposed stratigraphic layers. The acoustic classes representing fine sediments correlated with areas of a deeper SBP signal penetration.

We can summarize that dense MBES backscatter measurements offer the advantage of extracting angular responses from fine-scale seafloor patches without the need to perform backscatter mosaic segmentation. In this way, not only the spatial resolution of classification maps is improved but also the sedimentary classes are optimally separated. Future MBES survey planning may need to consider the acquisition of such high density of soundings per seafloor area, which would offer the possibility for accurate ARA-based seafloor classification on footprint-scale.

Acknowledgements We would like to specifically thank Sebastian Krastel (Institute of Geosciences, Christian-Albrechts-Universität, Kiel) and Christian Berndt (GEOMAR) for providing access to the MBES dataset collected in 2012. The SBP survey was supported by an Innomar Student Project which allowed us using the parametric SES-2000 sub-bottom profiler system with help by Peter Hümbs from Innomar. We would also like to thank, RV Littorina captain and crew, and Wärtsilä ELAC Nautik for providing a special pole for the SBP survey. Two anonymous reviewers are thanked as well as Dr. Geoffroy Lamarche for valuable comments and recommendations. We also thank Dr. Karin Meissner (Senckenberg) for providing the identification of macro-benthic organisms. Finally thanks go to Edna Hütten and Thomas J. Browning for providing valuable grammar and syntax corrections. This is publication 28 of the DeepSea Monitoring Group at GEOMAR.

Appendix

See Tables 4 and 5.

Table 4 Population statistic features and frequency distributions (x axis: backscatter (dB), y axis: frequency) of soundings from five sediment sample locations (5 × 5 m patches)

Training areas (5 × 5 m)	
	Distribution
Sample_no.: 1 Acoustic class: 5 Type: sandy gravel Number of soundings: 1517 Mean dB: −48.1	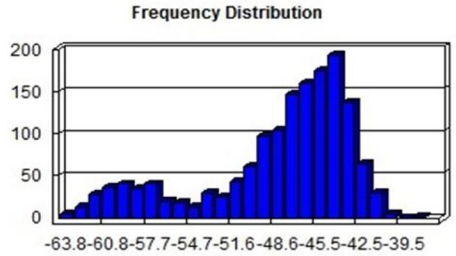
Sample_no.: 18 Acoustic class: 4 Type: gravelly sand Number of soundings: 1442 Mean dB: −53.9	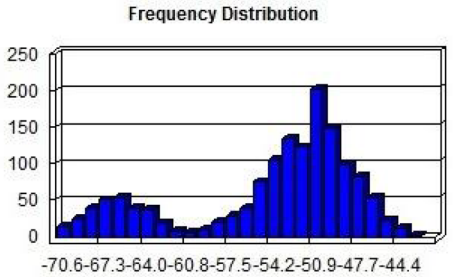
Sample_no.: 3 Acoustic class: 3 Type: sand Number of soundings: 782 Mean dB: −61.8	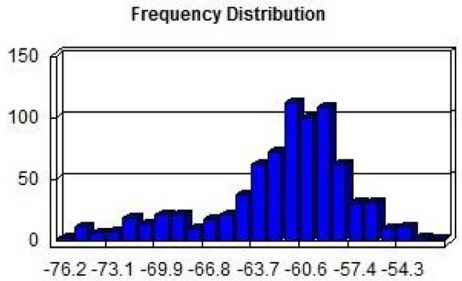
Sample_no.: 9 Acoustic class: 2 Type: (gravelly/sandy) mud Number of soundings: 312 Mean dB: −64.4	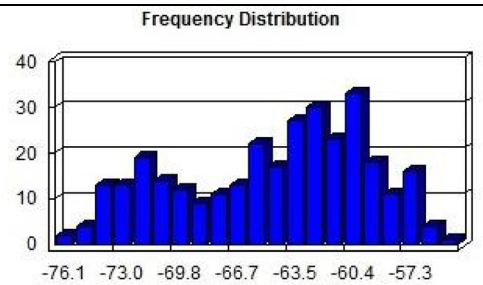
Sample_no.: 7 Acoustic class: 1 Type: mud and clay Number of soundings: 287 Mean dB: −71.7	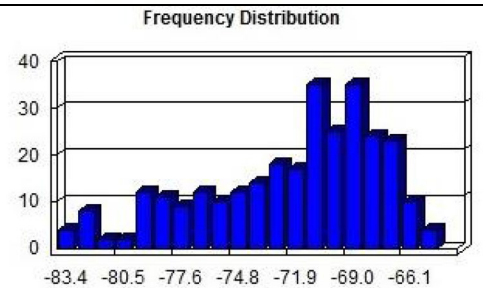

Table 5 Percentages and grain size statistics of the coarse and fine grain fractions, presence of shells from sieved data measurements and classifications results

Sample	W% >6.3 mm	W% 2–6.3 mm	W% 2 mm–500 µm	W% <500 µm	Shells/pebbles	d50 (<500 µm)	Mode (<500 µm)	D50 all (µm)	Mode all (µm)	Bayes class	ARA-MLC class	PCA class
1	14.59	20.17	34.12	31.12	1/1	240.0	246.0	2600	1000	5	5	5
2	2.23	30.89	21.96	44.91	1/1	220.0	246.0	1800	4000	5	5	5
3	0.00	0.65	14.49	84.86	1/0	170.0	197.0	210	180	3	3	3
4	0.00	0.49	2.56	96.95	1/0	151.8	191.5	200	180	3	3	3
5	0.00	0.69	3.28	96.03	1/0	41.3	73.0	100	90	2	3	2
6	0.00	0.00	0.00	100.00	0/0	23.0	44.3	50	40	2	1	2
7	0.00	0.00	0.00	100.00	0/0	23.0	43.5	50	40	1	2	1
8	0.00	0.00	0.00	100.00	0/0	26.3	43.0	50	40	1	1	1
9	0.00	3.39	0.74	95.87	0/0	20.8	41.0	40	40	3	2	2
10	0.00	0.00	0.72	99.28	0/0	21.0	43.8	40	40	2	2	2
11	0.00	0.72	0.24	99.04	0/0	20.5	42.0	50	40	2	–	–
12	0.00	0.42	15.36	84.21	1/1	197.0	236.0	320	250	4	5	4
13	0.00	0.27	7.89	91.84	1/0	157.0	270.0	290	250	3	3	3
14	0.00	0.38	21.87	77.76	1/1	192.0	216.0	280	180	3	3	3
15	0.00	0.40	4.08	95.52	1/0	206.0	236.0	220	130	3	3	3
16	0.00	0.07	7.94	92.00	1/1	236.0	246.0	460	350	3	3	4
17	0.00	8.06	18.38	73.57	0/1	84.0	188.0	210	180	4	3	4
18	0.00	1.41	31.15	67.44	1/0	282.0	270.0	270	350	4	4	4
19	0.00	0.00	7.93	92.07	0/0	226.0	236.0	310	250	3	3	3
20	0.00	0.13	5.90	93.97	0/0	56.0	258.0	280	250	3	2	3
21	0.00	1.10	3.87	95.04	0/0	112.0	150.0	150	130	4	4	4
22	0.00	0.00	1.31	98.69	0/0	50.8	109.0	110	90	2	3	2

References

Alevizos E, Snellen M, Simons DG, Siemes K, Greinert J (2015) Acoustic discrimination of relatively homogeneous fine sediments using Bayesian classification on MBES data. Mar Geol 370:31–42. doi:10.1016/j.margeo.2015.10.007, ISSN 0025-3227

Amiri-Simkooei AR, Snellen M, Simons DG (2009) River bed sediment classification using MBES backscatter data. J Acoust Soc Am 126(4):1724–1738

Amiri-Simkooei AR, Snellen M, Simons DG (2011) Principal component analysis of single-beam echo-sounder signal features for seafloor classification. IEEE J Ocean Eng 36:259, 272. doi:10.1109/JOE.2011.2122630

Benediktsson JA, Sveinsson JR, Arnason K (1995) Classification and feature extraction of AVIRIS data. IEEE Trans Geosci Remote Sens 33(5):1194–1205

Bentley SJ, Nittrouer CA, Sommerfield CK (1996) Development of sedimentary strata in Eckernförde Bay, southwestern Baltic Sea. Geo-Mar Lett 16:148–154. doi:10.1007/BF01204502

Beyer A, Chakraborty B, Schenke HW (2007) Seafloor characterization of the mound and channel provinces of the Porcupine Seabight: an application of the multi-beam angular backscatter data. Int J Earth Sci. doi:10.1007/s00531-005-0022-1

Blondel P, Huvenne V, Huehnerbach V (2006) Multi-frequency acoustics of deep-water coral habitats and textural characterisation. In: Jesus SN, Rodriguez OC (eds.) Proceedings of the 8th European conference on underwater acoustics, 12–15 Jun 2006. 8th European conference on underwater acoustics carvoeiro, Portugal, ECUA Secretariat, pp 379–384

Brown CJ, Blondel P (2009) The application of underwater acoustics to seabed habitat mapping, Appl Acoust 70(10):1241. doi:10.1016/j.apacoust.2008.09.006, ISSN 0003-682X

Brown CJ, Smith SJ, Lawton P, Anderson JT (2011) Benthic habitat mapping: a review of progress towards improved understanding of the spatial ecology of the seafloor using acoustic techniques. Estuar Coast Shelf Sci 92:502–520. doi:10.1016/j.ecss.2011.02.007

Calinski T, Harabasz J (1974) A dendrite method for cluster analysis. Commun Stat 3:1–27

Calvert J, Strong JA, Service M, McGonigle C, Quinn R (2014) An evaluation of supervised and unsupervised classification techniques for marine benthic habitat mapping using multibeam echosounder data. ICES J Mar Sci. doi:10.1093/icesjms/fsu223

Che Hasan R, Ierodiaconou D, Laurenson L (2012a) Combining angular response classification and backscatter imagery segmentation for benthic biological habitat mapping. Estuar Coast Shelf Sci 97:1–9

Che Hasan R, Ierodiaconou D, Monk J (2012b) Evaluation off our supervised learning methods for benthic habitat mapping using backscatter from multi-beam sonar. Remote Sens 4:3427–3443

Che Hasan R, Ierodiaconou D, Laurenson L, Schimel A (2014) Integrating multibeam backscatter angular response, mosaic and bathymetry data for benthic habitat mapping. PLoS ONE 9(5):e97339. doi:10.1371/journal.pone.0097339

Collier JS, Brown CJ (2005) Correlation of sidescan backscatter with grain size distribution of surficial seabed sediments. Mar Geol 214(4):431–449. doi:10.1016/j.margeo.2004.11.011

Eleftherakis D, Snellen M, Amiri-Simkooei A, Simons DG, Siemes K (2014) Observations regarding coarse sediment classification based on multi-beam echo-sounder's backscatter strength and depth residuals in Dutch rivers. J Acoust Soc Am 135(number 6):3305–3315

Erdey-Heydorn MD (2008) An ArcGIS seabed characterization toolbox developed for investigating benthic habitats. Mar Geodesy 31(4):318–358. doi:10.1080/01490410802466819

Fakiris E, Zoura D, Ferentinos G, Papatheodorou G (2014) Towards joint use of side scan sonar and subbottom profiler data for the automatic quantification of marine habitats. Case study: Lourdas gulf, Kefalonia isl., Greece, UA2014 2nd international conference and exhibition on underwater acoustics

Ferrini VL, Flood RD (2006) The effects of fine-scale surface roughness and grain size on 300 kHz multibeam backscatter intensity in sandy marine sedimentary environments. Mar Geol 228(1–4):153–172. doi:10.1016/j.margeo.2005.11.010

Folk RL (1954) The distinction between grain size and mineral composition in sedimentary-rock nomenclature. J Geol 62:344–359

Fonseca L, Mayer LA (2007) Remote estimation of surficial seafloor properties through the application angular range analysis to multibeam sonar data. Mar Geophys Res 28:119–126

Fonseca L, Brown C, Calder B, Mayer L, Rzhanov Y (2009) Angular range analysis of acoustic themes from Stanton Banks Ireland: a link between visual interpretation and multibeam echosounder angular signatures. Appl Acoust 70:1298–1304. doi:10.1016/j.apacoust.2008.09.008

Hamilton LJ, Parnum IM (2011) Acoustic seabed segmentation from direct statistical clustering of entire multibeam sonar backscatter curves. Cont Shelf Res 31:138–148

Hovland M, Judd AG (1988) Seabed pockmarks and seapages, impact on geology, and the marine environment. Graham and Trotman, London, p 293

Huang Z, Siwabessy J, Nichol S, Anderson T, Brooke B (2013) Predictive mapping of seabed cover types using angular response curves of multibeam backscatter data: testing different feature analysis techniques. Cont Shelf Res 61–62:12–22. doi:10.1016/j.csr.2013.04.024

Hughes Clarke JE (1994) Towards remote seafloor classification, using the angular response of acoustic backscatter: a case study from multiple overlapping GLORIA Data. IEEE J OceaN Eng 19:112–127

Ierodiaconou D, Burq S, Laurenson L, Reston M (2007) Marine habitat mapping using multibeam data, georeferenced video and image classification techniques: a case study in southwest Victoria. J Spatial Sci 52(1):93–104

Jensen JB, Kuijpers A, Bennike O, Laier T, Werner F (2002) New geological aspects for freshwater seepage and formation in Eckernförde Bay, western Baltic. Cont Shelf Res 22:2159–2173. doi:10.1016/S0278-4343(02)00076-6

Lamarche G, Lurton X, Verdier A-L, Augustin J-M (2011) Quantitative characterisation of seafloor substrate and bedforms using advanced processing of multibeam backscatter-application to Cook Strait, New Zealand. Cont Shelf Res, 31(2 suppl):S93–S109. doi:10.1016/j.csr.2010.06.001

Le Bas TP, Huvenne VAI (2009) Acquisition and processing of backscatter data for habitat mapping: comparison of multibeam and sidescan systems. Appl Acoust 70(10):1248–1257. doi:10.1016/j.apacoust.2008.07.010, ISSN 0003-682X

Lurton X, Lamarche G (eds) (2015) Backscatter measurements by seafloor-mapping sonars. Guidelines and Recommendations Geohab Report, p 200

McGonigle C, Collier JS (2014) Interlinking backscatter, grain size and benthic community structure. Estuar Coast Shelf Sci 147:123–136. doi:10.1016/j.ecss.2014.05.025

Müller H, von Dobeneck T, Nehmiz W, Hamer K (2011) Near-surface electromagnetic, rock magnetic, and geochemical fingerprinting of submarine freshwater seepage at Eckernförde Bay (SW Baltic Sea). Geo-Mar Lett 31(2):123–140. doi:10.1007/s00367-010-0220-0

Nittrouer CA, Lopez GR, Wright LD, Bentley SJ, D'Andrea AF, Friedrichs CT, Craig NI, Sommerfield CK (1998) Oceanographic processes and the preservation of sedimentary structure in

Eckernförde Bay, Baltic Sea. Cont Shelf Res 18(14–15):1689–1714. doi:10.1016/S0278-4343(98)00054-5, ISSN 0278-4343

Parnum IM (2007) Benthic habitat mapping using multibeam sonar systems. PhD thesis, Curtin University, Perth, p 208

Preston J (2009) Automated acoustic seabed classification of multibeam images of Stanton Banks. Appl Acoust 70(10):1277–1287. doi:10.1016/j.apacoust.2008.07.011

Rzhanov Y, Fonseca L, Mayer L (2012) Construction of seafloor thematic maps from multibeam acoustic backscatter angular response data. Comput Geosci 41:181–187. doi:10.1016/j.cageo.2011.09.001

Siemes K, Snellen M, Amiri Simkooei A, Simons DG, Hermand JP (2010) Predicting spatial variability of sediment properties from hydrographic data for geoacoustic inversion. IEEE J Oceanic Eng 35(4):766–778

Simons DG, Snellen M (2009) A Bayesian technique to seafloor classification using multi-beam echo-sounder backscatter data. Appl Acoust 70:1258–1268. http://dx.doi.org/10.1016/j.apacoust.2008.07.013

Snellen M, Eleftherakis D, Amiri-Simkooei A, Koomans RL, Simons DG (2013) An inter-comparison of sediment classification methods based on multi-beam echo-sounder backscatter and sediment natural radioactivity data. J Acoust Soc Am 134(2):959–970. doi:10.1121/1.4812858

Sweeney EM, Gardner JV, Johnson JE, Mayer LA (2012) Geological interpretation of a low-backscatter anomaly found on the New Jersey continental margin. Mar Geol 326–328:46–54. doi:10.1016/j.margeo.2012.08.007, ISSN 0025-3227

Verfaillie E, Degraer S, Schelfaut K, Willems W, Van Lancker V (2009) A protocol for classifying ecologically relevant marine zones, a statistical approach. Estuar Coast Shelf Sci 83(2):175–185. doi:10.1016/j.ecss.2009.03.003, ISSN 0272-7714

von Deimling JS, Weinrebe W, Tóth ZS, Fossing H, Endler R, Rehder G, Spieß V (2013) A low frequency multibeam assessment: spatial mapping of shallow gas by enhanced penetration and angular response anomaly. Mar Petrol Geol 44:217–222. doi:10.1016/j.marpetgeo.2013.02.013, ISSN 0264-8172

Whiticar MJ (2002) Diagenetic relationships of methanogenesis, nutrients, acoustic turbidity, pockmarks and freshwater seepages in Eckernförde Bay. Mar Geol 182:29–53. doi:10.1016/S0025-3227(01)00227-4